Journal of Catalysis 346 (2017) 117–124

Contents lists available at ScienceDirect

Journal of Catalysis

journal homepage: www.elsevier.com/locate/jcat

Glycerol electro-oxidation on bismuth-modified platinum single crystals

Amanda C. Garcia [a,b], Yuvraj Y. Birdja [a], Germano Tremiliosi-Filho [b], Marc T.M. Koper [a,*]

[a] Leiden Institute of Chemistry, Leiden University, PO Box 9502, 2300 RA Leiden, The Netherlands
[b] Instituto de Química de São Carlos, Universidade de São Paulo, Avenida Trabalhador São-Carlense 400, 13566-590 São Carlos, SP, Brazil

ARTICLE INFO

Article history:
Received 6 November 2016
Revised 19 December 2016
Accepted 20 December 2016
Available online 11 January 2017

Keywords:
Glycerol oxidation
Electrocatalysis
Platinum
Bismuth
Selectivity promoter

ABSTRACT

Herein we describe the role of Bi adatom irreversibly adsorbed on platinum single-crystal electrodes toward the oxidation of glycerol. Our results show that the presence of bismuth on the Pt(1 1 1) electrode improves the activity of the reaction, by preventing the adsorption of poisoning intermediates such as carbon monoxide, as well as the selectivity to dihydroxyacetone, while on the Pt(1 0 0)/Bi_{ir} electrode, the presence of a strongly bound glycerol-related adsorbate and a small amount of linearly bonded carbon monoxide causes a decrease in the activity. Significantly, the presence of bismuth on Pt(1 0 0) does not change its tendency to produce only glyceraldehyde as the primary product of the oxidation of glycerol. The increase in the selectivity to DHA on Pt(1 1 1)/Bi_{ir} is attributed to the interaction of the Bi adatom with the enediol intermediate, an adsorbed intermediate that exists on Pt(1 1 1) but not on Pt(1 0 0). The enediol is the key intermediate in the isomerization reaction between glyceraldehyde and dihydroxyacetone, and the stabilization of this intermediate by the interaction with the bismuth enhances the rate of the isomerization reaction toward the thermodynamically most stable isomer, namely dihydroxyacetone.

1. Introduction

The oxidation of organic compounds derived from biomass has attracted increasing attention due to its possible application in fuel cells and because some compounds can be used to produce valuable chemicals [1,2]. Glycerol, a surplus by-product from the production of biodiesel, can be oxidized to CO_2 yielding 14 electrons, making its use as fuel in a Direct Alcohol Fuel Cell (DAFC) very attractive [1,3]. Furthermore, glycerol can be oxidized to functionalized feedstock such as dihydroxyacetone (DHA), glyceric acid (GEA) and tartronic acid (TA), all commercially useful compounds [2]. DHA, a product of secondary alcohol oxidation, is especially interesting because it is widely used in the cosmetic industry as self-tanning agent. It is currently produced by microbial oxidation, a method that requires a low glycerol concentration and a long operation time [4].

Previous results have shown that glycerol can be converted into DHA by using an electrochemical approach [5,6]. Our recent work on Pt single crystal electrodes showed that the selectivity of the electrochemical oxidation of glycerol to DHA is sensitive to the surface structure and that this sensitivity is related to the initial mode through which glycerol binds to the surface, as also confirmed by Density Functional Theory calculations [6].

In heterogeneous catalysis several mono- and bi-metallic catalysts (Pd, Pt, Au and Pt—Bi, Au—Pt, Au—Ag) have been considered promising for the selective conversion of glycerol to DHA [7–9]. Also homogeneous catalysts have been reported for the selective glycerol oxidation to DHA [10].

It has been demonstrated that the modification of the surface composition of noble metal electrodes constitutes a convenient approach to enhance their electrocatalytic properties [11–13]. The deposition of a certain amount of adatoms can enhance the electrocatalytic activity of a given electrode and improve its selectivity. Specifically, the effect of the adsorption of p-block metal promoters, such as Bi and Sb, on Pt electrodes, toward the electro-oxidation of organic compounds such as formic acid and ethylene glycol has been widely studied [12–17].

More recently, Kwon et al. [5,18] showed that the electro-oxidation of glycerol to DHA can be achieved with almost 100% selectivity by making use of adatom species on a Pt/C electrode. It was observed that in the absence of promoters, the primary alcohol oxidation is dominant; however, with bismuth or antimony in solution, the oxidation of secondary hydroxyl groups is preferred. A similar selectivity enhancement was reported for the selective electro-oxidation of sorbitol (C6 polyol) to glucose and fructose [19].

However, the role of promoters, such as Bi, in enhancing the activity and selectivity of catalytic oxidation reactions is still not clear. Many works discuss the enhanced activity based on the

* Corresponding author.
E-mail address: m.koper@lic.leidenuniv.nl (M.T.M. Koper).

http://dx.doi.org/10.1016/j.jcat.2016.12.013
0021-9517/

so-called third-body effect, in which Bi blocks the formation of poisonous species during the oxidation of small organic molecules [11,20,21]. In addition, electronic and bifunctional catalytic effects have been suggested [22,23]. However, there is currently no good understanding of how Bi and Sb steer the selectivity of polyol oxidation.

This paper discusses the effect of irreversibly adsorbed bismuth (Bi_{ir}) on the activity and selectivity of glycerol oxidation on Pt single-crystal electrodes. Our results show that the presence of adatom does not change the pathway toward the oxidation of primary and secondary hydroxyl groups of the glycerol molecule, compared to the unmodified electrodes [6]. However, the presence of Bi on Pt(1 1 1) enhances the activity and selectivity to DHA, while on Pt(1 0 0), the presence of bismuth causes a decrease in the overall activity, although the efficiency to primary alcohol oxidation is improved. This observation gives important hints about the mechanism of the selectivity enhancement for glycerol oxidation by Bi and other p-block metal promoters.

2. Experimental section

2.1. Experimental conditions, electrodes and reactants

All experiments were carried out at room temperature (20° ± 1 °C) in a single classical three-electrode cell, which was cleaned by a standard procedure to remove all organic traces. For the preparation of the solutions, high-purity perchloric acid (70%, Merck Suprapur), glycerol (GLY) (85%, analytical grade), bismuth (III) oxide (98%, Sigma-Aldrich) and ultrapure water from a Millipore system (18.2 MΩ cm^{-1}) were used. The counter and reference electrodes were a Pt wire and a reversible hydrogen electrode (RHE), respectively. The working electrodes were Pt(1 1 1) and Pt (1 0 0) purchased from icryst, with a geometric area of 0.0402 and 0.0366 cm^2, respectively. Prior to each experiment, the working electrode was flame annealed and cooled down in a H_2 + Ar atmosphere, after which it was protected with a droplet of water saturated with the cooling gases to prevent the contamination and reconstruction of the surfaces during the transfer to the electrochemical cell [24]. Next the electrode was characterized in an O_2-free 0.5 M perchloric acid solution to ensure that the surface has been properly prepared and the cell and solution were completely clean.

The bismuth adlayer was prepared by an irreversible adsorption technique, which consists in bringing the electrode into contact with a Bi^{3+} containing solution (10^{-5}–10^{-4} M) at open circuit potential for different adsorption times [11]. By changing the immersion time, different Bi coverages can be achieved. According to the literature [11], the charge density associated with the surface process and the blockage of the hydrogen and anion adsorption reactions on the bare Pt sites are proportional. The adatom coverage of the surface (θ) was therefore estimated using the following equation:

$$\theta = \frac{Q_{Ad}}{nQ_{Pt(hkl)}}$$

where Q_{Ad} is the charge density involved in the adatom oxidation process, $Q_{Pt(hkl)}$ is the charge density corresponding to the transfer of one electron per Pt atom on the surface [241 μC cm^{-2} for Pt (1 1 1) and 209 μC cm^{-2} for Pt(1 0 0)], and n is the number of electrons transferred in the oxidation of one Bi adatom (i.e. $n = 3$) [11,25].

After preparation, the modified electrode was rinsed with ultrapure water and transferred to the electrochemical cell containing the supporting electrolyte (0.5 M $HClO_4$). The presence of irreversibly adsorbed bismuth on the Pt(1 1 1) and Pt(1 0 0) electrodes was investigated by cyclic voltammetry recorded from 0.05 to 0.9 V *vs.* RHE at 10 mV s^{-1}. The potential was controlled by a Potentiostat/galvanostat (μAutolab Type III). After characterization of the Bi coverage, the electrode was transferred to the cell containing a deaerated 0.1 M GLY + 0.5 M $HClO_4$ solution for the glycerol electro-oxidation measurements, with the potential scanned from 0.05 V to 0.9 V at 1.0 mV s^{-1}. For all the electrochemical experiments, prior to bringing the work electrode in contact with the solution, a potential of 0.1 V *vs.* RHE was applied.

For the adsorbate formation from glycerol on Pt(1 1 1)/Bi_{ir} and Pt(1 0 0)/Bi_{ir}, the electrode was held at 0.2 V *vs.* RHE with the working electrode immersed in the working electrolyte for 1 min. After adsorption, the electrode was rinsed in O_2 free ultrapure water to remove excess of alcohol and then transferred to another electrochemical cell, which contained the pure electrolyte (0.5 M $HClO_4$). CO stripping measurements were also performed on Pt(1 1 1)/Bi_{ir} and Pt(1 0 0)/Bi_{ir} for comparison with the adsorbate stripping. For these experiments, CO gas was bubbled during 5 min into the cell containing pure electrolyte with the potential kept at 0.1 V *vs.* RHE. Next, excess CO was removed from the solution by bubbling argon for 10 min. The oxidative stripping of the resulting adsorbates and CO was performed in a clean supporting electrolyte by sweeping potential between 0.06 V and 0.9 V at 10.0 mV s^{-1}.

2.2. HPLC experiments

High Performance Liquid Chromatography (HPLC) was used to detect the liquid products produced during the electrochemical oxidation of the glycerol [26]. The reaction products were collected during the cyclic voltammetry with a small Teflon tip (0.38 mm inner diameter) positioned close (10 μm) to the center of the electrode surface, which was connected to a PEEK capillary with inner/outer diameters of 0.13/1.59 mm. Before sample collection, the tip and capillary were cleaned with ultrapure water and supporting electrolyte. The sample volume collected in each well was 60 μL on a 96-well microtiter plate (270 μL/well, Screening Devices b. v.) using an automatic fraction collector (FRC-10A, Shimadzu). The flow rate of sample collection was adjusted to 60 μL/min with a Shimadzu pump (LC-20AT). After collecting samples, the microtiter plate was covered by a silicon mat to prevent the evaporation of collected samples. The samples were collected each 60 mV, in the potential range between 0.06 V and 0.9 V *vs.* RHE at 1.0 mV s^{-1} on Pt(1 1 1)/Bi_{ir} and Pt(1 0 0)/Bi_{ir} electrodes. The collected samples were analyzed by high-performance liquid chromatography (Prominence HPLC, Shimadzu). The microtiter plate with the collected samples was placed in an auto sampler (SIL-20A) holder and 30 μL of sample was injected into the column. The column configuration was an Aminex HPX 87-H (Bio-Rad) together with a Micro-Guard Cation H cartridge (Bio-Rad) in series with a Sugar SH1011 (Shodex) column and diluted sulfuric acid (0.5 mM) was used as the eluent. The temperature of the column was maintained at 70 °C in a column oven (CTO-20A), and the separated compounds were detected with a refractive index detector (RID-10A). The expected products were analyzed separately to produce standard calibration curves at 70 °C (i.e., glyceraldehyde, dihydroxyacetone, glyceric acid, glycolic acid, formic acid, oxalic acid, mesoxalic acid, hydroxypyruvic acid and tartronic acid).

2.3. OLEMS experiments

The volatile products of the reaction were detected using online electrochemical mass spectroscopy (OLEMS) with an evolution mass spectrometer system (European Spectrometry systems Ltd) [27]. The porous Teflon tip (inner diameter, 0.5 mm) was positioned close (≈10 μm) to the center of the electrode. Before the experiments, the tip was dipped into a 0.2 M $K_2Cr_2O_7$ in 2 M

H_2SO_4 solution for 15 min and rinsed with ultrapure water thoroughly. The gas products were collected through a polyether ether ketone (PEEK) capillary into the mass spectrometer. A 1500-V secondary electron multiplier (SEM) voltage was applied for all the fragments. The OLEMS measurement was conducted while the CV was scanned from 0.06 to 0.9 V and back at a scan rate of 1.0 mV s^{-1}.

2.4. FTIR experiments

To provide information about the surface-adsorbed intermediates of the electrochemical glycerol oxidation reaction, *in situ* FTIR spectra were collected. The FTIR instrument was a Bruker Vertex 80V IR spectrometer equipped with liquid nitrogen cooled detector. *In situ* FTIR experiments were performed in a three electrode spectro-electrochemical cell with a CaF_2 prism attached to the bottom of the cell. Details concerning the cell and the setup are described in the literature [28]. FTIR spectra were obtained in the wave number range between 2500 cm^{-1} and 1000 cm^{-1}. Spectra were collected in 0.1 V steps from 0.1 V to 0.9 V *vs*. RHE. They were computed from the average of 100 interferograms with spectral resolution set to 8 cm^{-1}. Spectra are presented as absorbance, according to $A = -\log(R/R_0)$, where R and R_0 are the reflectance corresponding to the single beam spectra obtained at the sample and reference potentials, respectively.

3. Results and discussion

Fig. 1 shows the voltammetric profiles of the Pt(1 1 1)/Bi_{ir} and Pt(1 0 0)/Bi_{ir} electrodes in 0.5 M $HClO_4$. The base voltammetry of the corresponding unmodified Pt(1 1 1) and Pt(1 0 0) electrodes, in the same solution, is shown as a reference. The profiles are very similar to those reported in the literature [29,30]. On the Pt(1 1 1) electrode (Fig. 1a), three different potential regions can be observed: the region between 0.05 and 0.4 V, which corresponds to the hydrogen adsorption/desorption region, the double layer region between 0.4 and 0.6 V and the so-called butterfly region (0.6 V < E < 0.9 V), which is commonly ascribed to the reversible adsorption of OH_{ad}. On the Pt(1 0 0) electrode (Fig. 1b), the hydrogen adsorption/desorption region, between 0.05 and 0.45 V, is directly followed by a region of OH_{ad} formation, with the formation of PtO_2 starting above 0.9 V [31].

The comparison of the cyclic voltammetry with the Bi-modified Pt(1 1 1) and Pt(1 0 0) electrodes shows that the presence of the adatom on the surface after irreversible deposition is evidenced by a significant suppression of the hydrogen and OH adsorption processes. On both electrodes, a new redox process takes place, giving rise to a peak couple. On Pt(1 1 1)/Bi_{ir}, the hydrogen region (suppressed with respect to the clean Pt(1 1 1)) is followed by a wide "double layer" potential range, and at higher potential a reversible peak centered at *ca.* 0.67 V is observed. There is no consensus regarding the exact nature of this peak. According to Clavilier et al. [32], the underlying process for these peaks is due to the Bi^0/Bi^{3+} surface redox process. However, Schmidt et al. [25] showed that Bi_{ir} remains in its zero-valent state over the whole potential range, by making use of *in situ* surface X-ray scattering in combination with *ex situ* X-ray photoelectron spectroscopy. Kim and Rhee have studied Bi on Pt(1 1 1) by electrochemical STM and did not observe the formation of ordered adlayers [33].

In the CV profile of the Pt(1 0 0)/Bi_{ir} electrode, the redox process of the bismuth adatoms takes place at a higher potential compared to Pt(1 1 1)/Bi_{ir} with a peak couple observed at ~0.88 V. On both Bi-modified surfaces, the voltammetric profile remains essentially reversible over the entire potential range, and unchanged during continuous cycling, indicating that the adatoms are stable on the surface. The comparison of the results shown in Fig. 1a and b reveals that the surface process is sensitive to the crystallographic orientation of the electrode surface. The coverage of Bi on both surfaces was calculated using equation (1), giving values of $\theta = 0.13$ and $\theta = 0.17$, for Pt(1 1 1)/Bi_{ir} and Pt(1 0 0)/Bi_{ir}, respectively.

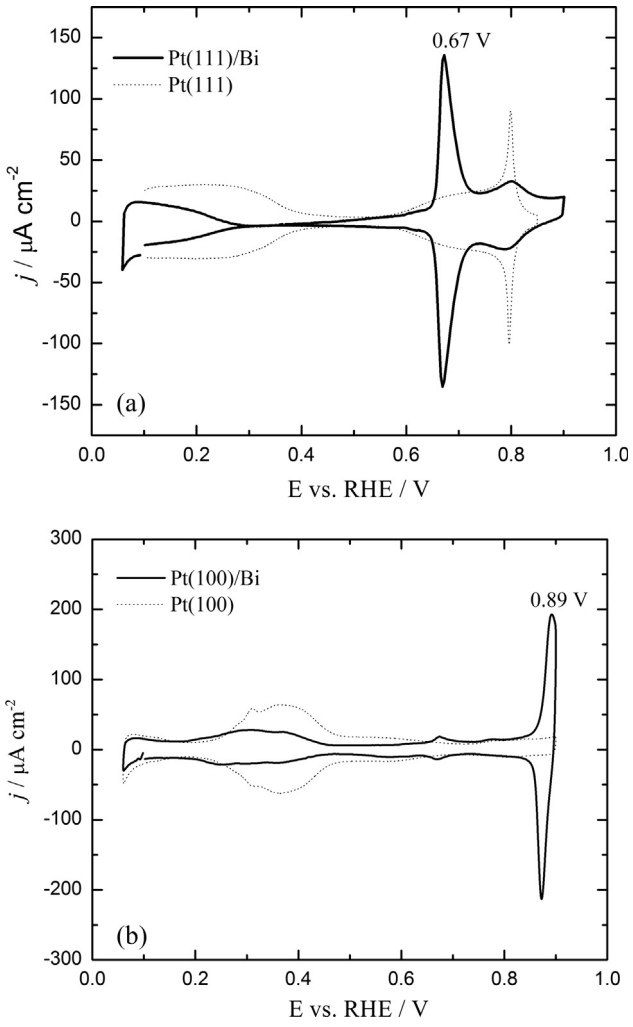

Fig. 1. Base voltammetry of (a) Pt(1 1 1) (dashed line) and Pt(1 1 1)/Bi_{ir} ($\theta = 0.13$, solid line) and (b) Pt(1 0 0) (dashed line) and Pt(1 0 0)/Bi_{ir} ($\theta = 0.17$, solid line), all in 0.5 M $HClO_4$ at 10 mV s^{-1}.

Fig. 2 shows the first scan for the oxidation of glycerol on the irreversibly adsorbed bismuth on Pt(1 1 1) and Pt(1 0 0) electrodes. For comparison, the profiles for unmodified Pt(1 1 1) and Pt(1 0 0) electrodes are also shown. The corresponding liquid products and the selectivity of the liquid products detected by *online* HPLC during the forward scan as well as the mass signal (m/z = 44) related to the production of CO_2 as measured by OLEMS are also displayed. Similar to the results obtained by Kwon et al. [5], which showed that a Bi-modified Pt/C electrode increases the activity for the glycerol oxidation compared to Pt/C, our results show that the presence of bismuth on the Pt(1 1 1) electrode causes an increase in the current density for glycerol oxidation compared to unmodified Pt (1 1 1) (dashed line) (Fig. 2a). Glycerol starts to be oxidized at *ca.* 0.58 V on Pt(1 1 1)/Bi_{ir}, *ca.* 30 mV more positive than on Pt(1 1 1). At around 0.68 V the current reaches a maximum followed by a drop in current due to the formation of surface hydroxide intermediates, which block the electrode surface. In the back potential scan, at *ca.* 0.8 V the surface is reactivated and at 0.68 V a peak current is observed.

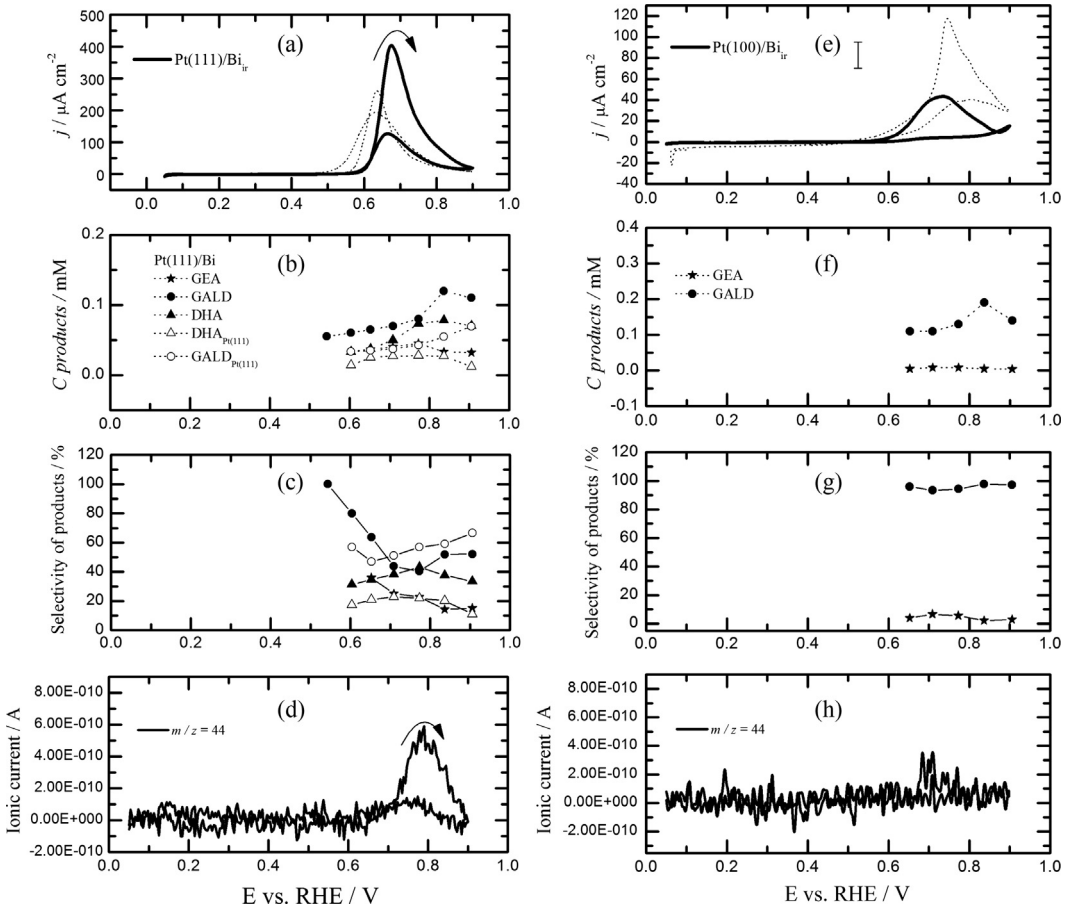

Fig. 2. Cyclic voltammograms for 0.1 M glycerol oxidation on (a) Pt(111)/Bi$_{ir}$ and (b) Pt(100)/Bi$_{ir}$ electrodes in $HClO_4$, at 1.0 mV s^{-1}. Corresponding liquid product concentration and selectivity of liquid products as measured by online HPLC on (b, c) Pt(111)/Bi$_{ir}$ and (f, g) Pt(100)/Bi$_{ir}$, and corresponding mass signal (m/z = 44) related to the production of CO_2 as measured by OLEMS on (d) Pt(111)/Bi$_{ir}$ and (h) Pt(100)/Bi$_{ir}$. Voltammetric profiles for glycerol oxidation on unmodified Pt(111) and Pt(100) (dashed line) are shown for comparison.

A qualitatively similar behavior is observed for Pt(100)/Bi$_{ir}$ electrode (Fig. 2e). The onset potential for the glycerol oxidation is around 0.6 V, the same potential as for the Pt(100) electrode. However, in the positive-going potential scan, the presence of bismuth shows a lower current density compared to clean Pt(100). In the negative-going potential scan, the peak related to the reactivation of the electrode is not observed, meaning that during the positive scan some species is formed that blocks the active sites and that is not removed in the negative-going scan.

Fig. 2(b, c) and (f, g) compare the corresponding liquid products and the selectivity of the various products of glycerol oxidation as measured by *online* HPLC for the Pt(111)/Bi$_{ir}$ and Pt(100)/Bi$_{ir}$ electrodes, respectively. Recently, we showed that the electrochemical oxidation of glycerol and its selectivity are very sensitive to the surface structure of the electrode [6], with Pt(111) surface being selective to the oxidation of both the primary and secondary alcohol, while the Pt(100) surface is selective only for the oxidation of the primary hydroxyl group. Similar results are observed here for the Bi-modified electrode. Specifically, the HPLC results show that the presence of irreversibly adsorbed bismuth on Pt(111) leads to a considerable increase in the concentration of glyceraldehyde (GALD) and dihydroxyacetone (DHA), products from the oxidation of the primary and secondary hydroxyl groups, respectively, whereas on Pt(100)/Bi$_{ir}$ an increase is observed in the concentrations of glyceraldehyde and glyceric acid compared with the unmodified Pt(100) surface [6]. A closer look further shows that on Pt(111)/Bi$_{ir}$, (Fig. 2b and c), GALD is formed initially at around 0.5 V, with no DHA detected. The production of DHA starts to be observed at around 0.65 V, leading to a peak in production and a selectivity of *ca.* 50% at around 0.7–0.8 V, with a corresponding minimum in selectivity for GALD (~40%). On the clean Pt(111) electrode, in the same potential range, the selectivity to DHA is significantly lower, around 20%. Glyceric acid (GEA) also was detected as a by-product of the oxidation of glycerol, and similar to the other products, its concentration increases in the presence of bismuth, compared to the unmodified electrode.

On the Pt(100)/Bi$_{ir}$ electrode, only the oxidation of the primary hydroxyl group takes place, as on unmodified Pt(100), leading to the production of glyceraldehyde, which is further oxidized to glyceric acid. According to Fig. 2f, GALD starts to be produced at around 0.65 V, leading to a peak at 0.8 V and a selectivity close to 90%. These results show that although the presence of bismuth on Pt(100) surface causes a loss in the overall activity of the reaction, it still contributes to an increase in the concentration of liquid products from the oxidation of the primary OH group.

By comparing the results shown in Fig. 2, we conclude that a low coverage of Bi on the modified Pt single-crystal electrodes leads to an increase in the formation of primary and secondary oxidation products, and on Pt(111) it leads to an increase in the selectivity toward DHA. However, on Pt(100), the presence of Bi has no effect on the selectivity of the oxidation in terms of primary *vs.* secondary alcohol. In other words, the effect of Bi on the enhanced secondary alcohol oxidation is restricted to the (111) surface. Therefore, Bi seems to change the balance in the pathways

between primary and secondary alcohol oxidation, rather than open up a new pathway.

Cyclic voltammetry combined with OLEMS measurements was also performed, in order to detect the CO_2 production from the oxidation of glycerol. The results illustrated in Fig. 2d show that the electrochemical oxidation of glycerol on Pt(1 1 1)/Bi_{ir} is accompanied by the production of CO_2, while on Pt(1 0 0)/Bi_{ir} electrode (Fig. 2h), only a very small mass signal (m/z = 44) from CO_2 was detected. For both electrodes, the production of CO_2 appears suppressed with respect to the unmodified Pt(1 1 1) and Pt(1 0 0) electrodes [6]. The peak in CO_2 formation is about 0.1 V more positive than the current peak (Fig. 2a), which we believe is due to the fact that CO_2 is not the first and the main product of the glycerol oxidation on Pt(1 1 1)/Bi_{irr}.

It has been discussed in the literature that bismuth hinders the formation of the carbon monoxide poison on the platinum surface through a third-body effect [34,35]. In order to obtain more insight into the blocking effect of the adatom on the Pt surfaces, we performed some adsorbate-stripping measurements. The results are shown in Fig. 3a and b. The blank profiles for the Bi-modified electrodes are also shown for comparison. In our previous paper [6], we showed that during the stripping of the adspecies coming from glycerol adsorption, an oxidation stripping peak was observed, on both Pt(1 1 1) and Pt(1 0 0) electrodes. This adspecies corresponds to an adsorbed intermediate that is difficult to oxidize but that is not CO. However, on both bismuth modified-Pt electrodes, no such oxidation peak was observed in the potential range considered. On Pt(1 1 1)/Bi_{ir} (Fig. 3a), we observe that after the adsorption of glycerol, the hydrogen region remains almost the same, while the peak at *ca.* 0.67 V broadens somewhat and lowers in intensity. Additionally, in the back scan, the peak was shifted to slightly lower potential. These results suggest that a possible adsorbate causes a small modification of the Bi-Pt(1 1 1) sites but no significant blockage. On Pt(1 0 0)/Bi (Fig. 3b), on the other hand, the results show that the hydrogen region is totally suppressed by the presence of an adsorbate. Moreover, the redox peak related to the Bi at around 0.88 V is also inhibited, suggesting that the species from glycerol adsorbs not only on the Pt(1 0 0) sites but interacts with the Bi—Pt(1 0 0) sites, similar to what has been observed for formic acid oxidation on Pt(1 0 0)/Bi_{ir} [34].

The "stripping" of adspecies from glycerol adsorption can be compared with the CO stripping from both Pt(1 1 1)/Bi_{ir} and Pt(1 0 0)/Bi_{ir} surfaces, as shown in Fig. 3c and d, respectively. On both Pt(1 1 1)/Bi_{ir} and Pt(1 0 0)/Bi_{ir} electrodes, the voltammetric stripping profiles of the CO adlayer show a complete blocking of the hydrogen adsorption/desorption region, since no significant current is observed in the potential range between 0.05 and 0.4 V. On the Pt(1 1 1)/Bi_{ir} electrode, in the positive-going potential scan, it is possible to observe two peaks at 0.67 and 0.73 V and they are related to the surface redox process of bismuth and to CO oxidation on Pt(1 1 1) sites [36–38], respectively. On Pt(1 0 0)/Bi, at higher potential a CO stripping peak is observed at around 0.77 V, followed by peak couple at ~0.88 V related to the Bi redox process. Note that the Bi redox peaks on both platinum surfaces are smaller compared to those in Fig. 1, suggesting that CO may have displaced some of the adsorbed bismuth. Comparing to the results shown in Fig. 3a and b, we conclude that the GLY-related adsorbate on both Pt(1 1 1)/Bi_{ir} and Pt(1 0 0)/Bi_{ir} electrodes is not CO. Furthermore, the GLY-adsorbate seems to poison the Pt(1 0 0)/Bi_{ir} more than Pt(1 1 1)/Bi_{ir} surface, which could also explain the low activity of the Pt(1 0 0)/Bi_{ir} electrode in the back scan in Fig. 2e.

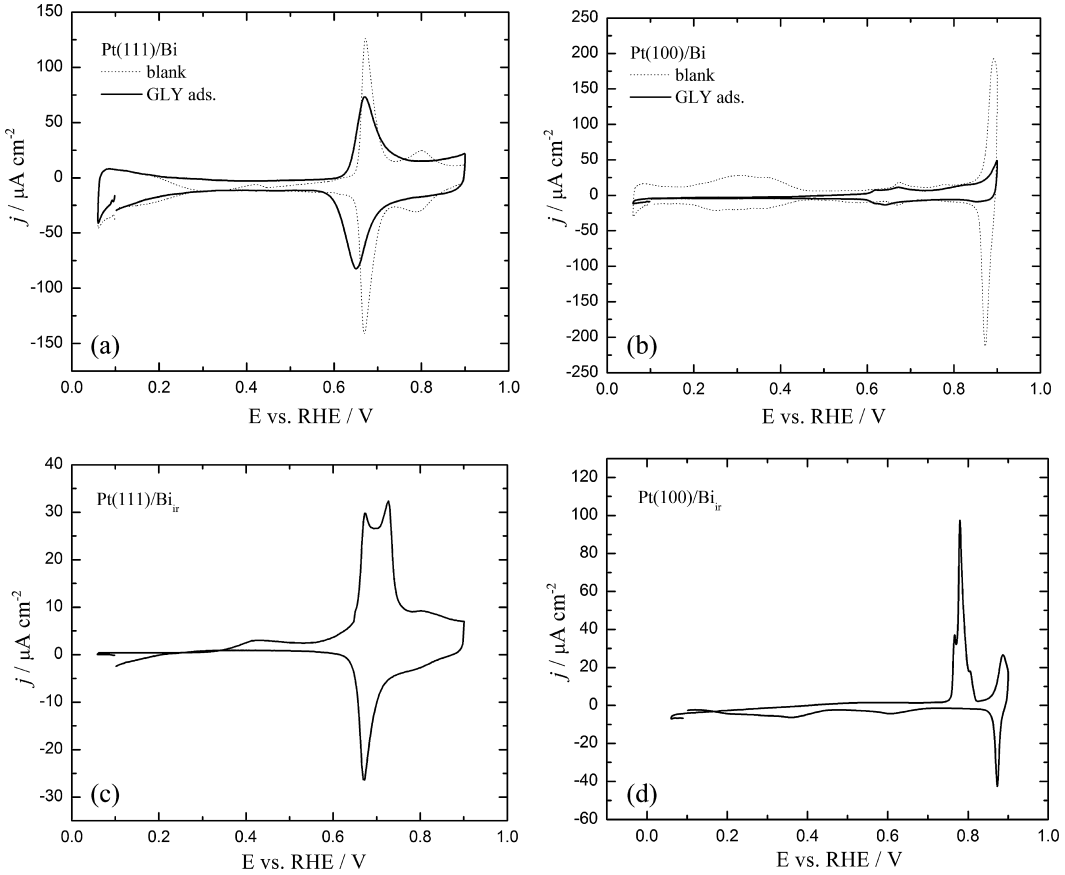

Fig. 3. Adsorbate stripping from glycerol adsorption on (a) Pt(1 1 1)/Bi_{ir} (θ = 0.13) and (b) Pt(1 0 0)/Bi_{ir} (θ = 0.17) electrodes and the corresponding CO stripping profiles (c, d) obtained by bubbling CO gas during 5 min in 0.5 M $HClO_4$; scan rate = 10 mV s^{-1}.

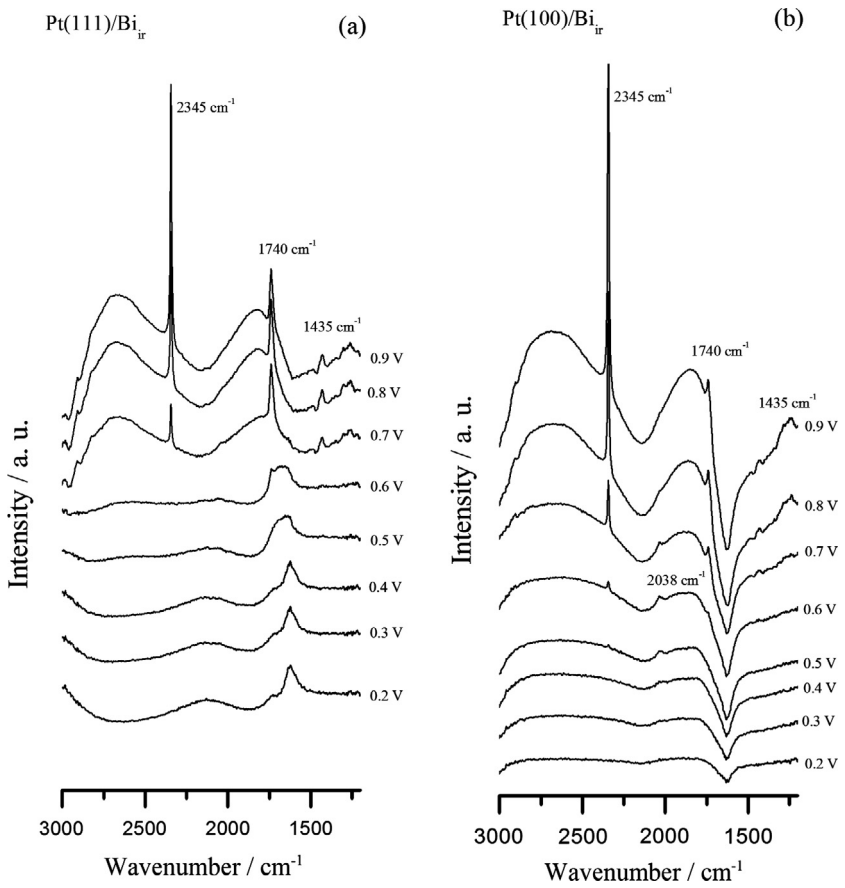

Fig. 4. *In situ* FTIR spectra as a function of potential (100 scans, resolution 8 cm^{-1}) of (a) Pt(111)/Bi$_{ir}$ and (b) Pt(100)/Bi$_{ir}$ in 0.5 M $HClO_4$ + 0.1 M glycerol. The reference spectra were collected at 0.1 V vs. RHE and the sample spectra were acquired by applying potential steps.

To investigate this blocking effect of Bi on Pt single crystals, *in situ* FTIR measurements were performed on both Pt(111)/Bi$_{ir}$ and Pt(100)/Bi$_{ir}$ electrodes. The main interest in these measurements is to compare any possible differences in the adsorbed species generated on the Pt surfaces during the glycerol oxidation in the presence of Bi with the results obtained for the unmodified Pt single crystals [6].

The spectra obtained as a function of the applied potential are displayed in Fig. 4. In our previous paper, it was observed that linearly and bridge-bonded adsorbed CO were detected on Pt(100) while on Pt(111) only linearly bonded CO was detected by *in situ* FTIR as adsorbed intermediates of the oxidation of glycerol [6]. Different features are observed for both Pt(111)/Bi$_{ir}$ and Pt(100)/Bi$_{ir}$ electrodes. On Pt(111)/Bi$_{ir}$ (Fig. 4a), the spectra acquired by increasing the potential show that the formation of linearly bonded CO is completely suppressed, since no band at around 2040 cm^{-1} was observed [39]. However, the band at 2345 cm^{-1}, assigned to the O—C—O asymmetric stretching mode of the CO_2 molecule [40], evidences the production of carbon dioxide at high potentials (0.7 V), in agreement with the OLEMS results in Fig. 2d. On Pt(100)/Bi$_{ir}$ the weak band at 2038 cm^{-1} is ascribable to the build-up of linearly bonded adsorbed carbon monoxide, which starts appearing at 0.5 V. The production of CO_2 starts at 0.6 V. At 0.8 V this linearly bonded CO has been completely oxidized to CO_2, since no band at 2038 cm^{-1} is observed anymore. The results suggest that the presence of the adatom blocks the sites responsible for the adsorption of the bridge-bonded CO, as observed for the unmodified Pt(100) electrode [6], but not the sites for linearly bonded CO. Similar behavior was observed for the formic acid oxidation on Bi-modified Pt(100), on which only the linearly bonded CO was detected as adsorbed intermediate in the range potential considered, while on clean Pt(100) electrode, both linearly and bridge bonded CO were detected as intermediate of the reaction [41–43].

On both electrodes, at 0.7 V two bands were observed at around 1740 and 1435 cm^{-1} assigned to the C=O stretching of carbonyl compounds and to the C—O stretching/OH deformation of carboxylic acids [44], respectively. These bands are related to the production of aldehydes, ketones and carboxylic acid. By comparison with a standard solution, the band at 1740 cm^{-1} can be attributed to formic acid. Indeed, previous works showed that during the electrochemical oxidation of glycerol, formic acid is one of the by-products of the reaction [5,6,45].

Formic acid oxidation leads to the formation of CO_2; however, it can also give rise to the formation of adsorbed carbon monoxide through dehydration. Based on the *in situ* FTIR spectra, we propose that Bi on the Pt(111) surface blocks the formation of adsorbed CO from formic acid, which is directly oxidized to CO_2. On the other hand, Bi on Pt(100) surface blocks only the adsorption of bridge-bonded CO, meaning that the production of CO_2 can be related to the oxidation of linearly bonded CO, in agreement with the literature [41]. However, there is still a contribution of the direct formic acid oxidation, because at 0.8 V (Fig. 4b) the band related to the linearly bonded CO has completely disappeared but CO_2 is still formed.

4. General discussion

Many works have discussed the role of p-block metal promoters, such as bismuth, on the catalytic oxidation of organic molecules on metal catalysts based on the idea that Bi blocks the

formation of poison from the oxidation of small organic compounds [17,34,41,46]. However, to understand how the presence of Bi^{3+} impacts on the selectivity of glycerol oxidation, we must invoke specific interactions of Bi^{3+} adatom with glycerol or one of its oxidation intermediates.

The main conclusion of our comparative study between the Bi^{3+}-promoted oxidation of glycerol on Pt(111) and Pt(100) is that the presence of Bi^{3+} does not introduce a new pathway to lead to the secondary alcohol oxidation, but rather it interacts with an already existing pathway on Pt(111) to favor the formation of dihydroxyacetone. In our previous paper [6] we ascribed the ability of Pt(111) to produce both glyceraldehyde and dihydroxyacetone to the presence of an adsorbed enediol-type intermediate. This intermediate was shown to be the most stable intermediate on Pt(111), in contrast to Pt(100), on which the most stable intermediate interacts through a single primary carbon. The enediol can isomerize to yield both glyceraldehyde and dihydroxyacetone. It is known that metal cations such as zinc or calcium can catalyze the isomerization reaction by interacting specifically with the enediol-type intermediate of the isomerization mechanism [47,48]. Since dihydroxyacetone is thermodynamically more stable than glyceraldehyde, by *ca.* 7.7 kJ mol^{-1} in the carbohydrate metabolism (equilibrium between GALD-phosphate and DHA-phosphate) [49], and by *ca.* 2.7 kJ mol^{-1} according to recent DFT calculations of Cheng et al. [48], catalyzing the isomerization reaction will yield more dihydroxyacetone. Therefore, we suggest that Bi^{3+} on the surface of Pt(111) interacts with the enediol, an intermediate of initial glycerol dehydrogenation on the Pt surface (see Fig. 5), catalyzing the isomerization to DHA, and explaining the increase in the concentration of DHA on the Bi-modified Pt(111) electrode. Such an enediol intermediate is much less stable on Pt (100), and for this reason DHA is not identified as a product of glycerol electro-oxidation on Pt(100)/Bi_{ir}. However, on the Pt (100) electrode, the presence of Bi leads to a strongly adsorbed GLY-adsorbate, which blocks the surface of the electrode and that is difficult to oxidize in the whole range potential, as demonstrated by the results of adsorbate stripping. Such a strongly bound GLY-adsorbate was not observed on Pt(111)/Bi_{ir}, suggesting that Bi on Pt(111) blocks both the adsorption of the poison from glycerol oxidation and also the adsorption of carbon monoxide from the dehydration of formic acid. On the other hand, on Pt(100)/Bi_{ir} the oxidation of formic acid leads to linearly adsorbed carbon monoxide, in addition to the GLY-adsorbate.

The results presented in this paper give insight into how Bi adatoms on the Pt surface enhance the secondary alcohol oxidation in glycerol. However, we note that the presence of a low coverage of Bi on Pt(111) does not lead to an almost complete shift in the selectivity from glyceraldehyde to dihydroxyacetone, which is the influence that (dissolved) Bi has on the electrocatalytic oxidation of glycerol on a carbon-supported nanoparticulate platinum catalyst [5]. In terms of the role of bismuth proposed in the previous paragraph, this would imply that under those conditions, the isomerization would be completely equilibrated to its most stable isomer, namely dihydroxyacetone.

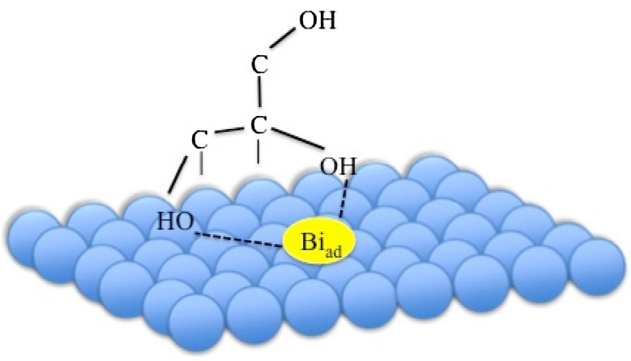

Fig. 5. Schematic representation of the proposed interaction of the enediol intermediate with Bi on Pt(111) surface. The exact state of Bi_{ad} on the surface depends on potential and pH [32].

5. Conclusion

In this paper we have studied the role of Bi adatoms on the improvement of activity and selectivity of the oxidation of glycerol on platinum single crystal electrodes. We found that the presence of bismuth on the Pt(111) electrode improves both the activity of the reaction and the selectivity to dihydroxyacetone, while on Pt (100) electrode the presence of bismuth causes a decrease in the activity and does not change the tendency of the Pt(100) surface to produce only glyceraldehyde. The role of Bi in the oxidation of glycerol is at least twofold. On Pt(111), Bi blocks sites preventing the adsorption of poisoning intermediates such as carbon monoxide, leading to a higher activity. On Pt(100) the presence of Bi reduces only partially the amount of poison formed during the reaction, as our stripping experiments and *in situ* FTIR results show the presence of a strongly bound glycerol-related adsorbate and a small amount of linearly bonded carbon monoxide. Secondly, and more importantly, we attribute the increase in the selectivity to DHA on Pt(111)/Bi_{ir} to the interaction of the Bi adatom with the enediol intermediate, an adsorbed intermediate that exists on Pt (111) but not on Pt(100) [6]. The enediol is the key intermediate in the isomerization reaction between glyceraldehyde and dihydroxyacetone, and the stabilization of this intermediate by the interaction with the bismuth enhances the rate of the isomerization reaction toward the thermodynamically most stable isomer, namely dihydroxyacetone.

Acknowledgments

A.C.G and G.T.F. acknowledge financial support from the São Paulo Research Foundation from Brazil (project no. 2014/24438-8 and 2012/10856-7). A.C.G and M.T.M.K. also acknowledge the Holland Research School of Molecular Chemistry (HRSMC) for financial support.

References

[1] M. Simões, S. Baranton, C. Coutanceau, Electro-oxidation of glycerol at Pd based nano-catalysts for an application in alkaline fuel cells for chemicals and energy cogeneration, Appl. Catal. B Environ. 93 (2010) 354–362, http://dx.doi.org/10.1016/j.apcatb.2009.10.008.

[2] M. Pagliaro, R. Ciriminna, H. Kimura, M. Rossi, C. Della Pina, From glycerol to value-added products, Angew. Chem. Int. Ed. (2007) 4434–4440, http://dx.doi.org/10.1002/anie.200604694.

[3] C.-H. Zhou, J.N. Beltramini, Y.-X. Fan, G.Q. Lu, Chemoselective catalytic conversion of glycerol as a biorenewable source to valuable commodity chemicals, Chem. Soc. Rev. 37 (2008) 527–549, http://dx.doi.org/10.1039/b707343g.

[4] B. Katryniok, H. Kimura, E. Skrzynska, J-S. Girardon, P. Fongarland, M. Capron, R. Ducoumlombier, N. Mimura, S. Paul, F. Dumeignil, Selective catalytic oxidation of glycerol: perspectives for high value chemicals, Green Chem. 13 (2011) 1960–1979, http://dx.doi.org/10.1039/c1gc15320j.

[5] Y. Kwon, Y. Birdja, I. Spanos, P. Rodriguez, M.T.M. Koper, Highly selective electro-oxidation of glycerol to dihydroxyacetone on platinum in the presence of bismuth, ACS Catal. 2 (2012) 759–764, http://dx.doi.org/10.1021/cs200599g.

[6] A.C. Garcia, M.J. Kolb, C. Van Nierop, Y. Sanchez, J. Vos, Y.Y. Birdja, Y. Kwon, et al., Strong impact of platinum surface structure on primary and secondary alcohol oxidation during electro-oxidation of glycerol, ACS Catal. 6 (2016) 4491–4500, http://dx.doi.org/10.1021/acscatal.6b00709.

[7] H. Kimura, Selective oxidation of glycerol on a platinum-bismuth catalyst by using a fixed bed reactor, Appl. Catal. A Gen. 105 (1993) 147–158, http://dx.doi.org/10.1016/0926-860X(93)80245-L.

[8] S. Demirel, K. Lehnert, M. Lucas, P. Claus, Use of renewables for the production of chemicals: glycerol oxidation over carbon supported gold catalysts, Appl. Catal. B Environ. 70 (2007) 637–643, http://dx.doi.org/10.1016/j.apcatb.2005.11.036.

[9] A. Brandner, P. Claus, Platinum - Bismuth-Catalyzed Oxidation of Glycerol: Kinetics and the Origin of Selective Deactivation, J. Phys. Chem. (2010) 1164–1172.
[10] R.M. Painter, D.M. Pearson, R.M. Waymouth, Selective catalytic oxidation of glycerol to dihydroxyacetone, Angew. Chem. – Int. Ed. 49 (2010) 9456–9459, http://dx.doi.org/10.1002/anie.201004063.
[11] V. Climent, N. Garcia-Araez, J.M. Feliu, Clues for the molecular level understanding of electrocatalysis on single-crystal platinum surfaces modified by p-bolck adatoms, in: M.T.M. Koper (Ed.), Fuel Cell Catal. A Surf. Sci. Approach, Wiley, Hoboken, New Jersey, 2009, pp. 209–244.
[12] S. Motoo, M. Watanabe, Electrocatalysis by ad-atoms: part IV. Enhancement of the oxidation of formic acid on Pt-Au(subs) and Au-Pt(subs) electrodes by bismuth adatoms, J. Electroanal. Chem. Interfacial Electrochem. 98 (1979) 203–211, http://dx.doi.org/10.1016/S0022-0728(79)80260-0.
[13] A. Fernandez-Vega, J.M. Feliu, A. Aldaz, J. Clavilier, Heterogeneous electrocatalysis on well defined platinum surfaces modified by controlled amounts of irreversibly adsobed adatoms. Part {II}. Formic acid oxidation on the Pt(100) Bi system, J. Electroanal. Chem. 258 (1989) 101, http://dx.doi.org/10.1016/0022-0728(89)87130-X.
[14] J. Clavilier, J.M. Feliu, A. Fernandez-Vega, A. Aldaz, Electrochemical behaviour of irreversibly adsorbed bismuth on Pt (100) with different degrees of crystalline surface order, J. Electroanal. Chem. Interfacial Electrochem. 269 (1989) 175–189, http://dx.doi.org/10.1016/0022-0728(89)80111-1.
[15] E. Herrero, J.M. Feliu, A. Aldaz, Poison formation reaction from formic acid on Pt(100) electrodes modified by irreversibly adsorbed bismuth and antimony, J. Electroanal. Chem. 368 (1994) 101–108, http://dx.doi.org/10.1016/0022-0728(93)03032-K.
[16] E. Herrero, M.J. Llorca, J.M. Feliu, A. Aldaz, Oxidation of formic acid on Pt(100) electrodes modified by irreversibly adsorbed tellurium, J. Electroanal. Chem. 383 (1995) 145–154, http://dx.doi.org/10.1016/0022-0728(94)03721-E.
[17] E. Herrero, J.M. Feliu, A. Aldaz, CO adsorption and oxidation on Pt(111) electrodes modified by irreversibly adsorbed bismuth in sulfuric acid medium, J. Catal. 152 (1995) 264–274, http://dx.doi.org/10.1006/jcat.1995.1081.
[18] Y. Know, T.J.P. Hersbach, M.T.M. Koper, Electro-oxidation of glycerol on platinum modified by adatoms: activity and selectivity effects, Top. Catal. 57 (2014) 1272–1276, http://dx.doi.org/10.1007/s11244-014-0292-6.
[19] Y. Kwon, K.J.P. Schouten, J.C. Van Der Waal, E. De Jong, M.T.M. Koper, Electrocatalytic conversion of furanic compounds electrocatalytic conversion of furanic compounds, ACS Catal. 6 (2016) 6704–6717, http://dx.doi.org/10.1021/acscatal.6b01861.
[20] M. Besson, P. Gallezot, Selective oxidation of alcohols and aldehydes on metal catalysts, Catal. Today 57 (2000) 127–141, http://dx.doi.org/10.1016/S0920-5861(99)00315-6.
[21] T.J. Schmidt, R.J. Behm, B.N. Grgur, N.M. Markovic, P.N. Ross, Formic acid oxidation on pure and Bi-modified Pt(111): temperature effects, Langmuir 16 (2000) 8159–8166, http://dx.doi.org/10.1021/la000339z.
[22] E. Christoffersen, P. Liu, A. Ruban, H. Skriver, J. Nørskov, Anode materials for low-temperature fuel cells: a density functional theory study, J. Catal. 199 (2001) 123–131, http://dx.doi.org/10.1006/jcat.2000.3136.
[23] S. Lee, S. Mukerjee, E. Ticianelli, J. McBreen, Electrocatalysis of CO tolerance in hydrogen oxidation reaction in PEM fuel cells, Electrochim. Acta 44 (1999) 3283–3293, http://dx.doi.org/10.1016/S0013-4686(99)00052-3.
[24] J. Clavilier, R. Faure, G. Guinet, R. Durand, Preparation of monocrystalline Pt microelectrodes and electrochemical study of the plane surfaces cut in the direction of the 111 and 110 planes, J. Electroanal. Chem. Interfacial Electrochem. 107 (1979) 205–209, http://dx.doi.org/10.1016/S0022-0728(79)80022-4.
[25] T.J. Schmidt, V.R. Stamenkovic, A. Lucas, M. Nenad, P.N. Ross, Surface processes and electrocatalysis on the Pt (hkl)/Bi-solution interface, Phys. Chem. Chem. Phys. 3 (2001) 3879–3890, http://dx.doi.org/10.1039/b102388h.
[26] Y. Kwon, M.T.M. Koper, Combining voltammetry with HPLC: application to electro-oxidation of glycerol, Anal. Chem. 82 (2010) 5420–5424, http://dx.doi.org/10.1021/ac101058t.
[27] A.H. Wonders, T.H.M. Housmans, V. Rosca, M.T.M. Koper, On-line mass spectrometry system for measurements at single-crystal electrodes in hanging meniscus configuration, J. Appl. Electrochem. 36 (2006) 1215–1221, http://dx.doi.org/10.1007/s10800-006-9173-4.
[28] G. Garcıa, P. Rodrıguez, V. Rosca, M.T.M. Koper, Fourier transform infrared spectroscopy study of CO electro-oxidation on Pt (111) in alkaline media, Langmuir 25 (2009) 13661–13666, http://dx.doi.org/10.1021/la902251z.
[29] A. Rodes, M.A. Zamakhchari, K. El Achi, J. Clavilier, Electrochemical behaviour of Pt(100) in various acidic media, J. Electroanal. Chem. Interfacial Electrochem. 305 (1991) 115–129, http://dx.doi.org/10.1016/0022-0728(91)85206-5.
[30] J. Clavilier, R. Albalat, R. Gomez, J.M. Orts, J.M. Feliu, A. Aldaz, Study of the charge displacement at constant potential during CO adsorption on Pt(110) and Pt(111) electrodes in contact with a perchloric acid solution, J. Electroanal. Chem. 330 (1992) 489–497, http://dx.doi.org/10.1016/0022-0728(92)80326-Y.
[31] Y.-F. Huang, P.J. Kooyman, M.T.M. Koper, Intermediate stages of electrochemical oxidation of single-crystalline platinum revealed by in situ Raman spectroscopy, Nat. Commun. 7 (2016), http://dx.doi.org/10.1038/ncomms12440.
[32] J. Clavilier, J.M. Feliu, A. Aldaz, An irreversible structure sensitive adsorption step in bismuth underpotential deposition at platinum electrodes, J. Electroanal. Chem. Interfacial Electrochem. 243 (1988) 419–433, http://dx.doi.org/10.1016/0022-0728(88)80045-7.
[33] J. Kim, C.K. Rhee, Structural evolution of irreversibly adsorbed Bi on Pt(111) under potential excursion, J. Solid State Electrochem. 17 (2013) 3109–3114, http://dx.doi.org/10.1007/s10008-013-2218-9.
[34] A. Fernandez-Vega, J.M. Feliu, A. Aldaz, J. Clavilier, Heterogeneous electrocatalysis on well defined platinum surfaces modified by controlled amounts of irreversibly adsobed adatoms. Part {II}. Formic acid oxidation on the Pt(100) Bi system, J. Electroanal. Chem. 261 (1989) 113–125, 0022-0728/89.
[35] A. Ferre-Vilaplana, J.V. Perales-Rondón, J.M. Feliu, E. Herrero, Understanding the effect of the adatoms in the formic acid oxidation mechanism on Pt(111) electrodes, ACS Catal. 5 (2015) 645–654, http://dx.doi.org/10.1021/cs501729j.
[36] A. Cuesta, A. Couto, A. Rincón, M.C. Pérez, A. López-Cudero, C. Gutiérrez, Potential dependence of the saturation CO coverage of Pt electrodes: the origin of the pre-peak in CO-stripping voltammograms. Part 3: Pt(poly), J. Electroanal. Chem. 586 (2006) 184–195, http://dx.doi.org/10.1016/j.jelechem.2005.10.006.
[37] N.P. Lebedeva, M.T.M. Koper, J.M. Feliu, R.A. Van Santen, Mechanism and kinetics of the electrochemical CO adlayer oxidation on Pt(111), J. Electroanal. Chem. 524 (2002) 242–251, http://dx.doi.org/10.1016/S0022-0728(02)00669-1.
[38] N.P. Lebedeva, A. Rodes, J.M. Feliu, M.T.M. Koper, R.A. Van Santen, Role of crystalline defects in electrocatalysis: CO adsorption and oxidation on stepped platinum electrodes as studied by in situ infrared spectroscopy, J. Phys. Chem. B. 106 (2002) 9863–9872, http://dx.doi.org/10.1021/jp0203806.
[39] M. Avramov-Ivic, J.-M. Léger, B. Beden, F. Hahn, C. Lamy, Adsorption of glycerol on platinum in alkaline medium: effect of the electrode structure, J. Electroanal. Chem. 351 (1993) 285–297, http://dx.doi.org/10.1016/0022-0728(93)80240-I.
[40] D.Z. Jeffery, G.A. Camara, The formation of carbon dioxide during glycerol electrooxidation in alkaline media: first spectroscopic evidences, Electrochem. Commun. 12 (2010) 1129–1132, http://dx.doi.org/10.1016/j.elecom.2010.06.001.
[41] S.-C. Chang, Y. Ho, M.J. Weaver, Applications of real-time infrared spectroscopy to electrocatalysis at bimetallic surfaces. I. Electrooxidation of formic acid and methanol on bismuth-modified Pt(111) and Pt(100), Surf. Sci. 265 (1992) 81–94, http://dx.doi.org/10.1016/0039-6028(92)90489-S.
[42] S.G. Sun, J. Clavilier, A. Bewick, The mechanism of electrocatalytic oxidation of formic acid on Pt(100) and Pt(111) in sulphuric acid solution: an EMIRS study, J. Electroanal. Chem. 240 (1988) 147–159.
[43] S.-C. Chang, L.-W.H. Leung, M.J. Weaver, Metal crystallinity effects in electrocatalysis as probed by real-time FTIR spectroscopy: electrooxidation of formic acid, methanol, and ethanol on ordered low-index platinum surfaces, J. Phys. Chem. 94 (1990) 6013–6021, http://dx.doi.org/10.1021/j100378a072.
[44] J.L. Bott-Neto, A.C. Garcia, V.L. Oliveira, N.E. de Souza, G. Tremiliosi-Filho, Au/C catalysts prepared by a green method towards C3 alcohol electrooxidation: a cyclic voltammetry and in situ FTIR spectroscopy study, J. Electroanal. Chem. 735 (2014) 57–62, http://dx.doi.org/10.1016/j.jelechem.2014.10.010.
[45] Y. Kwon, K.J.P. Schouten, M.T.M. Koper, Mechanism of the catalytic oxidation of glycerol on polycrystalline gold and platinum electrodes, Chemcatchem 3 (2011) 1176–1185, http://dx.doi.org/10.1002/cctc.201100023.
[46] J. Clavilier, S.G. Sun, Electrochemical study of the chemisorbed species formed from formic-acid dissociation at platinum single-crystal electrodes, J. Electroanal. Chem. 199 (1986) 471–480, http://dx.doi.org/10.1016/0022-0728(86)80021-3.
[47] R.W. Nagorski, J.P. Richard, Mechanistic imperatives for aldose - Ketose isomerization in water: specific, general base- and metal ion-catalyzed isomerization of glyceraldehyde with proton and hydride transfer, J. Am. Chem. Soc. 123 (2001) 794–802, http://dx.doi.org/10.1021/ja003433a.
[48] L. Cheng, C. Doubleday, R. Breslow, Evidence for tunneling in base-catalyzed isomerization of glyceraldehyde to dihydroxyacetone by hydride shift under formose conditions, Proc. Natl. Acad. Sci. USA 112 (2015) 4218–4220, http://dx.doi.org/10.1073/pnas.1503739112.
[49] M. Yudkin, R. Offord, A Guidebook to Biochemistry, Cambridge University Press, 1980.